

Crossover in the scaling of island size and capture zone distributions

T. J. Oliveira^{1,(a)} and F. D. A. Aarão Reis^{2,(b)} *

¹ *Departamento de Física, Universidade Federal de Viçosa,
36570-000, Viçosa, MG, Brazil*

² *Instituto de Física, Universidade Federal Fluminense,
Avenida Litorânea s/n, 24210-340 Niterói RJ, Brazil*

(Dated: August 9, 2012)

Simulations of irreversible growth of extended (fractal and square) islands with critical island sizes $i = 1$ and 2 are performed in broad ranges of coverage θ and diffusion-to-deposition ratios R in order to investigate scaling of island size and capture zone area distributions (ISD, CZD). Large θ and small R lead to a crossover from the CZD predicted by the theory of Pimpinelli and Einstein (PE), with Gaussian right tail, to CZD with simple exponential decays. The corresponding ISD also cross over from Gaussian or faster decays to simple exponential ones. For fractal islands, these features are explained by changes in the island growth kinetics, from a competition for capture of diffusing adatoms (PE scaling) to aggregation of adatoms with effectively irrelevant diffusion, which is characteristic of random sequential adsorption (RSA) without surface diffusion. This interpretation is confirmed by studying the crossover with similar CZ areas (of order 100 sites) in a model with freezing of diffusing adatoms that corresponds to $i = 0$. For square islands, deviations from PE predictions appear for coverages near $\theta = 0.2$ and are mainly related to island coalescence. Our results show that the range of applicability of the PE theory is narrow, thus observing the predicted Gaussian tail of CZD may be difficult in real systems.

PACS numbers: 68.43.Hn, 05.40.-a, 68.35.Fx, 81.15.Aa

I. INTRODUCTION

The theoretical study of thin film and multilayer growth attracted much interest in the last decades motivated by the increasing number of experimental techniques and applications¹⁻³. Film morphology is strongly connected to the initial stages of its growth, where islands of various shapes may be formed. The submonolayer regime, in which a single incomplete layer is being formed, was modeled by various authors and is still the focus of much debate^{1,4-12}. The theoretical approaches usually try to explain the island size distributions (ISD) and the capture zone distributions (CZD), with a capture zone (CZ) defined as the area in which a diffusing adatom is more likely to attach to a given island than to any other one. The models were originally proposed for atomic epitaxy and recently extended to growth of other materials, such as organic molecule islands, colloidal epitaxy, and graphene epitaxy¹³⁻¹⁸.

For irreversible island growth, the most recent advance in the field is the theory of Pimpinelli and Einstein (PE)⁸, which proposed that CZD are described by the Wigner surmise (WS) from random matrix theory¹⁹. The basis of PE theory is the competition of CZs for aggregation of diffusing adatoms. Deviations in the peaks of simulated CZD and the WS were reported for point islands on surfaces⁹. However, a recent work showed excellent collapse of most CZD with the WS after suitable rescal-

ing, for point, fractal, and square islands, and showed that all CZD had the universal Gaussian decay predicted by PE¹². Indeed, that theory obtains the WS from a Langevin equation, which is expected to apply only for large CZs. Moreover, the tail of the ISD was predicted by a scaling approach that assumes the Gaussian decay of CZD and accounts for the island shape¹².

On the other hand, failure of the predicted decay of CZD was observed for point islands in one-dimensional lattices, where a decay as $\exp(-x^3)$ is found²⁰⁻²². This decay is also predicted analytically in two dimensions under a circular-cell approximation for CZs²³. For the more realistic cases of extended islands, there are additional reasons to expect limitations of the PE theory. First, as θ increases, the size of island-free regions decreases, enhancing the correlations between stable islands and consequently changing their competition dynamics. Moreover, if the diffusion-to-deposition ratio $R \equiv D/F$ is small, the diffusion lengths of the free adatoms are small, facilitating formation of new islands instead of capture by the existing ones.

This work is devoted to study the crossover from PE submonolayer growth (Gaussian CZD and related forms of ISD) in those conditions.

Simulations of irreversible growth of fractal and square islands with critical island nucleus of sizes $i = 1$ and 2 are performed with broad ranges of θ and R . There is a variety of shapes of CZD and ISD for small CZ areas and small islands (left tails of CZD and ISD). On the other hand, the right tails of CZD and ISD always show a crossover to simple exponential decay for small R or large θ . In some cases, it restricts the PE prediction to a narrow ranges of those variables.

*a) Email address: tiago@ufv.br

b) Email address: reis@if.uff.br

Those deviations are related to the decrease of the size of free regions between the islands, which become very close and strongly correlated, ruling out the (mean-field) PE theory that neglects island correlations. For small R , the exponential tail is an effect of small diffusion lengths of adatoms before aggregation, typical of random distributions of non-mobile adatoms, which is the random sequential adsorption (RSA) problem^{24,25}. As θ increases, for any R , fractal islands become large, thus most of the atoms are deposited near their branches and rapidly aggregated. Again, adatom diffusion lengths are small and RSA scaling appears. A CZ area reduction to less than 100 sites is characteristic of this crossover region. This is confirmed by results of a model with $i = 0$ where diffusing adatoms may stop moving without aggregating to an existing island (adatom freezing)⁶. The crossover in square island models as θ increases and the islands begin to coalesce is interpreted along the same lines.

The study of ISD and CZD is also important for experimental work²⁶⁻²⁹, particularly to determine the critical island size that reveals basic features of the aggregation processes. At this point, we note that recent works compared CZD and ISD with fitting curves including the WS, such as para-sexiphenyl island growth on different substrates^{30,31}, Cu deposition with impurities³², pentacene island growth with impurities¹⁷, $InAs$ quantum dot growth on $GaAs$ ³³, and C_{60} deposition on SiO_2 films¹⁸.

The rest of this work is organized as follows. In Sec. II, we present the growth models and summarize previous theoretical results. In Sec. III, we discuss the scaling of CZD and ISD of fractal islands for broad ranges of coverage and diffusion-to-deposition ratio, with special emphasis on deviations from PE predictions. In Sec. IV, the discussion is extended to square islands models. In Sec. V, we analyze a model where diffusing adatoms may freeze, which presents a crossover from regimes with relevant and irrelevant adatom diffusion. Sec. VI summarizes our results and presents our conclusions.

II. MODEL DEFINITION AND THEORETICAL APPROACHES

We consider models of atom deposition and diffusion on a square lattice with irreversible aggregation to islands larger than a critical size i . Atoms incide at randomly chosen lattice sites with rate F (number of deposited atoms per unit time per lattice site). An atom adsorbs at the incidence site only if it is empty, thus growth is restricted to a single layer. An adatom diffuses with coefficient D (number of random steps to neighboring sites per unit time) if it is not aggregated to a stable island. The critical nucleus i is the maximum size of a non-stable island, i. e. an island from which atoms can detach. Islands of size $i + 1$ or larger are stable.

The diffusion-to-deposition ratio is defined as $R \equiv D/F$. The coverage θ is defined as the ratio between

the number of adsorbed atoms and the number of lattice sites.

In fractal island models, each atom permanently aggregates at the site where it collides with a stable island. Since there is no relaxation of the aggregated atoms, branched shapes are produced, resembling those of diffusion-limited aggregation³⁴.

In square island models, after aggregation to a stable island, the atom instantaneously relaxes to a position that preserves the compact (square) shape³⁵. However, when two neighboring islands coalesce, they evolve independently: an atom aggregated at the border of one of the coalesced islands relaxes to a site in the border of that island to preserve its square shape.

In the case of point island models, all atoms of an island aggregate on a single lattice site. However, this case is not studied in this work, since our aim is to study features of extended islands.

It is reasonable to assume that the probability density of CZ area x follows the scaling form

$$P(x) = \frac{1}{\langle x \rangle} f\left(\frac{x}{\langle x \rangle}\right), \quad (1)$$

where f is a scaling function. An equivalent scaling form applies to the density of islands of size s , $Q(s)$. A recent work¹² proposed the scaling of CZD with the variance $\sigma_x \equiv \overline{(x - \langle x \rangle)^2}^{1/2}$ as

$$P(x) = \frac{1}{\sigma_x} g\left(\frac{x - \langle x \rangle}{\sigma_x}\right). \quad (2)$$

This procedure is inspired in the successful application to roughness distributions of thin film growth models^{36,37}. An equivalent form also applies to $Q(s)$.

In 1995, Amar and Family (AF) proposed the empirical formula for the ISD⁶

$$f_i(u) = C_i u^i \exp\left(-i a_i u^{1/a_i}\right), \quad (3)$$

where $u \equiv s/\langle s \rangle$ and C_i and a_i are normalization constants. This formula is widely used to fit experimental data²⁶⁻²⁹. Subsequently, Mulheran and Blackman (MB) proposed to relate the ISD to distributions of areas of Voronoi polygons and provided results close to those of point island models⁷. In all those works, comparison with simulation or experimental data focused on the peaks of the distributions.

A recent work by Körner et al³⁸ proposed mean-field rate equations accounting for coverage-dependent capture numbers and obtained good agreement with the peaks and the tails of the ISD for fractal islands. However, the theoretical ISD were obtained by numerical integration of those equations, thus the tail decays were not analyzed.

Recently, a significant advance was the proposal⁸ that CZD are described by the WS

$$P_\beta(z) = a_\beta z^\beta \exp(-b_\beta z^2), \quad (4)$$

where $z \equiv x / \langle x \rangle$, $\beta = \frac{2}{d}(i+1)$, d is the substrate dimension ($d = 2$ in the present work) and the parameters a_β and b_β are determined by normalization conditions. The PE theory is justified by a phenomenological argument that the CZD can be extracted from a Langevin equation representing the competition of neighboring islands for adatom aggregation.

Ref.¹² showed that the CZD scaling using Eq. (2) agrees with the WS of Eq. (4) for large values of R (typically $R \geq 10^7$) and small coverages, in point, fractal, and square island models. In all cases, the Gaussian right tail predicted by PE [Eq. (4)] was present. For point and square islands, some deviations in the left tails and in the peaks of the CZD appeared. However, deviations for small islands and small CZs are expected because the continuous approach of PE applies to large island and large CZ kinetics.

Ref.¹² considered $\beta = i + 1$ in the WS, as originally suggested⁸. The successful comparison is probably due to the adopted rescaling and contrasts to the proposal $\beta = i + 2$ of Refs.^{9–11}. The Gaussian decay also differs from the $\exp(-x^3)$ decay predicted in Ref.²³ for point islands, probably due to the use of a circular-cell approximation for CZs in that work.

A scaling approach predicts the decay of the right tails of ISD from the Gaussian tail of the CZD¹². For fractal islands, the decay is $\exp(-s^{4/D_F}) \approx \exp(-s^{2.36})$, where $D_F \approx 1.694$ ³⁹ is the fractal dimension of DLA clusters; for square islands, the ISD decay is also Gaussian. These results also agree with simulation data for large R and small coverages¹².

PE theory applies to systems where distant and large islands compete for aggregation of diffusing adatoms. The opposite situation is that of totally non-mobile adatoms, which is the random sequential adsorption (RSA) problem without diffusion^{24,25}. In this case, atoms irreversibly stick to the site where they are adsorbed. ISD and CZD have simple exponential decays⁴⁰ as

$$Q(s) \sim \exp(-s/\langle s \rangle). \quad (5)$$

III. DISTRIBUTIONS FOR FRACTAL ISLANDS

A. Simulation results

We performed simulations in lattices of very large lateral size, typically $L = 2048$, with R ranging between 10^4 and 10^9 , coverages up to $\theta = 0.4$, and critical nucleus $i = 1$ and $i = 2$. For $i = 2$, no energy barrier is considered for the dissociation of islands with two atoms.

In Fig. 1a, we show scaled CZD for $R = 10^9$ and various coverages, to be compared with the WS. The data for small coverage ($\theta = 0.1$ in Fig. 1a) is well fit by the WS, as previously shown in Ref.¹². However, deviations clearly appear for the largest coverages ($\theta = 0.3$ and 0.4) and a simple exponential decay of the right tail is found, in contrast to the Gaussian decay of the WS.

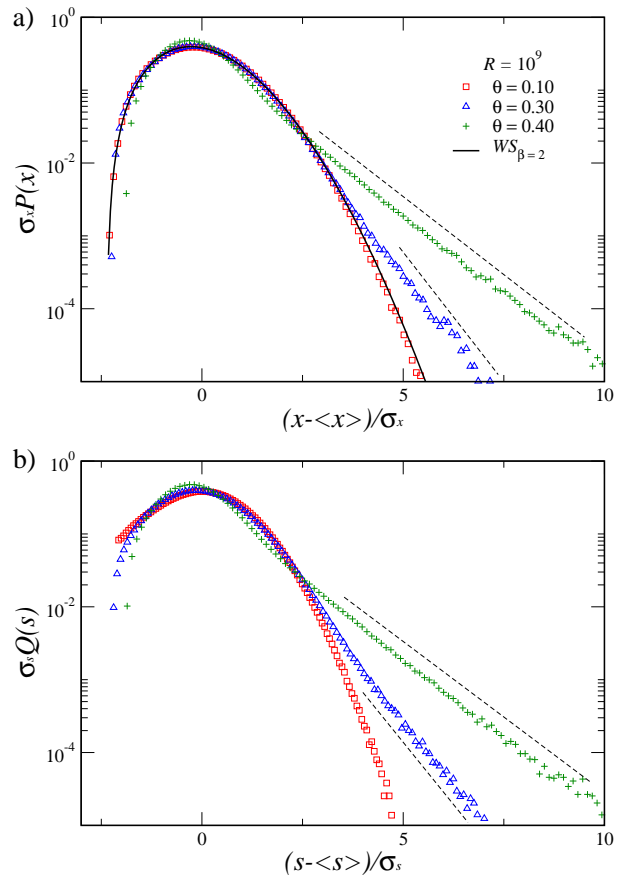


FIG. 1: (Color online) Scaled CZD (a) and ISD (b) for fractal islands with $i = 1$, $R = 10^9$ and several coverages. The solid line is the WS with $\beta = 2$. Dashed lines in all plots are guides to the eye.

In Fig. 1b, we show ISD for the same set of parameters. For small coverages, the right tail decay is slightly faster than a Gaussian, as discussed in Sec. II (see also Ref.¹²). However, it also crosses over to simple exponential decay for the largest coverages ($\theta = 0.3$ and 0.4).

The same crossover is found as R decreases, for fixed θ . In Fig. 2a, we show CZD for $\theta = 0.10$ and several values of R . The CZD for $R = 10^8$ agrees very well with the WS. However, the CZD for smaller values of R deviate from the WS and these deviations are enhanced for decreasing R . The simple exponential decay is found for large CZs for $R \lesssim 10^5$. Despite the deviation in the tails, for $R = 10^6$, the peak of the CZD still shows reasonable agreement with the WS (inset of Fig. 2a). For smaller R , the peaks also deviate from the WS, compensating the large difference in the tails.

In Fig. 2b, we show CZD for $\theta = 0.3$ and several values of R . For $R = 10^9$, the CZD agrees with the WS in two orders of magnitude around the peak [$\sigma_z P(z) \sim 10^{-2.5}$ to $10^{-0.5}$]. For smaller values of R , the fit covers a smaller region of the scaled CZD. The simple exponential decay of the right tail is observed for large CZs in all cases. The corresponding ISD are shown in Fig. 2c and also

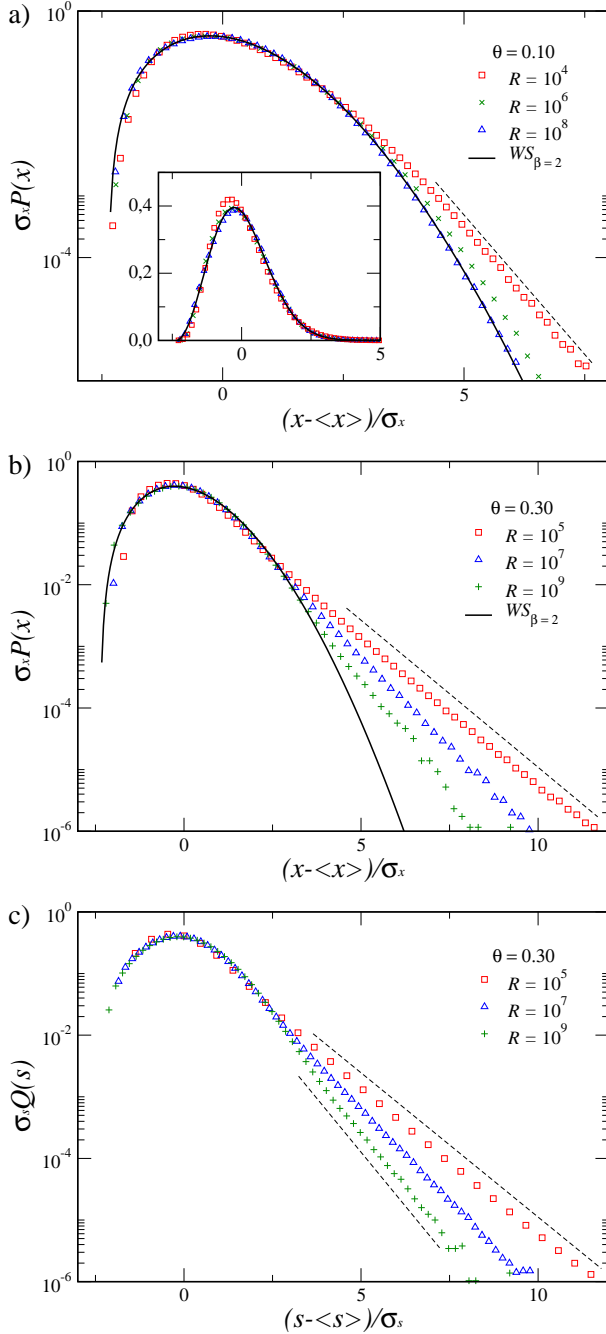


FIG. 2: (Color online) (a) Scaled CZD for fractal islands with $i = 1$, $\theta = 0.10$ and several ratios R . The inset in (a) shows the same data of the main plot in linear-linear scale. Scaled CZD (b) and ISD (c) for fractal islands with $i = 1$, $\theta = 0.30$ and several ratios R . The solid line is the WS with $\beta = 2$. Dashed lines in all plots are guides to the eye.

have that decay.

Note that coverage $\theta = 0.3$ is typical of many experimental works because islands become sufficiently large and facilitate microscopy investigation with a focus on island statistics. Moreover, $R \lesssim 10^5$ is typical of low temperatures, where island relaxation is difficult and the

fractal island model is realistic. These features suggest that experimental observation of PE predictions [particularly the Gaussian tail of CZD and the related form of the ISD (Sec. II)] will be difficult when large fractal islands are grown.

Fig. 3 shows images of the submonolayers grown with $R = 10^7$ and $R = 10^9$. For $\theta = 0.1$ and $R = 10^9$, the clusters are distant from their neighbors, i. e. there are large areas between them. The PE theory actually applies to this situation¹². However, for $R = 10^7$ and the same coverage, islands are much smaller, the distance between them decreases and the free areas around them are smaller. Under these conditions, the hypothesis of PE theory begin to fail. For $\theta = 0.1$ and $R = 10^6$, these effects are enhanced, which explains deviations of the CZD from the WS, as shown in Fig. 2a.

B. Interpretation of results

First we consider the deviations from PE scaling observed for small values of R .

In this case, the average adatom diffusion length $\langle l_D \rangle$ is very small, as well as its average diffusing time $\langle t_D \rangle$. Island growth mainly proceeds by incidence of new atoms very close to existing islands or very close to a diffusing adatom. If the lattice size is rescaled by $\langle l_D \rangle$ and time is rescaled by $\langle t_D \rangle$, then the islands of the rescaled lattice will grow by attachment of atoms deposited at neighboring sites, i. e. non-diffusion atoms. This leads to distributions with right tails (large islands) similar to RSA (Eq. 5).

Another important aspect to explain the deviations from PE scaling for small R is the small average island size and small average CZ area, since that theory follows from continuous approaches suitable for large CZs.

This interpretation helps to quantify the deviation of the DCZ from the WS as R decreases.

The deviation occurs for a CZ area x^* in which the WS decay $\exp[-(x/\langle x \rangle)^2]$ (Eqs. 1 and 4), matches the simple exponential decay of Eq. 5. Thus $x^* \sim \langle x \rangle$. In the crossover, islands are large and very close (see e. g. Fig. 3), branched but not fractal, thus the CZ area x^* is of the same order of the average island size. The dependence of this size on R and θ in the steady state of island growth is predicted by rate equation theory^{1,41-43} as $\langle s \rangle \sim R^{i/(i+2)} \theta^{-(i+1)/(i+2)}$. This gives

$$x^* \sim R^{i/(i+2)} \theta^{-(i+1)/(i+2)}. \quad (6)$$

The crossover area was determined in the simulated CZD as the point in which the tail changes its concavity in a log-linear plot. Error bars were estimated as the whole range of x that covers the crossover region. Fig. 4 shows the scaling of x^* with R , for fixed $\theta = 0.3$, with linear fits giving scaling exponents $\chi = 0.33 \pm 0.02$ for $i = 1$ and $\chi = 0.47 \pm 0.03$ for $i = 2$. This result is in good agreement with the predictions $x^* \sim R^{1/3}$ and

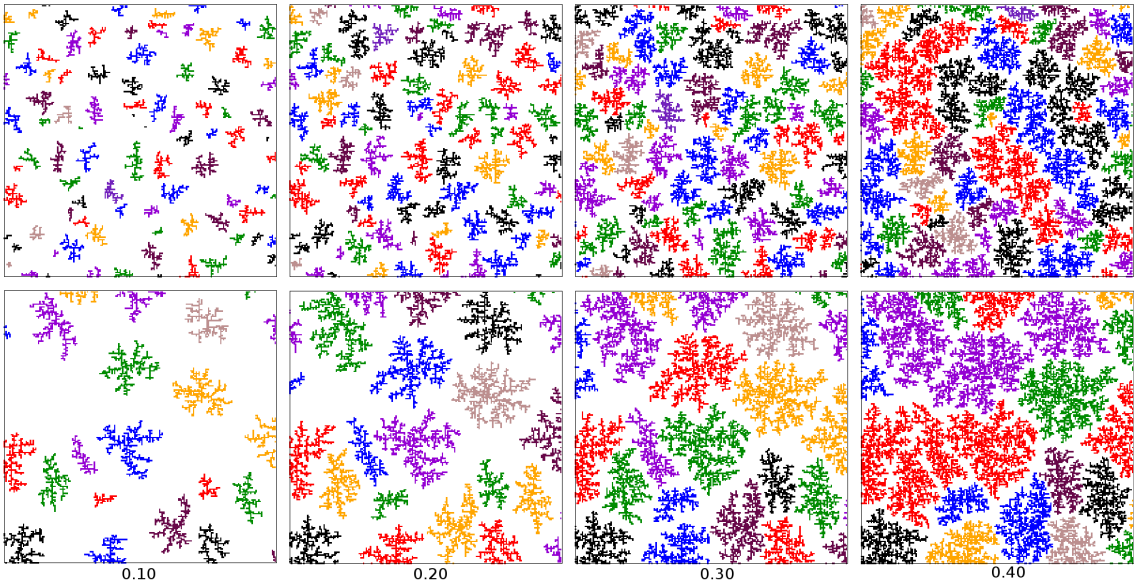


FIG. 3: (Color online) Fractal islands for several coverages with $R = 10^7$ (top) and $R = 10^9$ (bottom). The panels of lateral size 200 sites are cut from a system of size $L = 2048$.

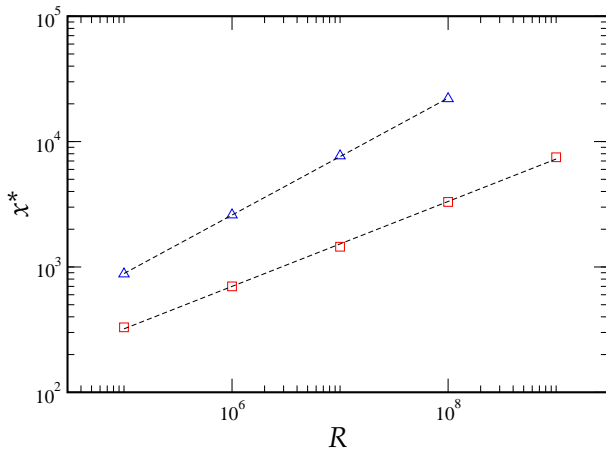


FIG. 4: (Color online) CZ crossover area x^* as a function of R , for $\theta = 0.30$ and critical islands sizes $i = 1$ (squares, red) and $i = 2$ (triangle, blue). The error bars are of the same order of the point size. Dashed lines are least squares fits of the data.

$x^* \sim R^{1/2}$ of Eq. (6) for $i = 1$ and 2, respectively. The scaling of the average island size at the crossover, s^* , is analogous to x^* , and was also confirmed numerically (results not shown).

Another interesting conclusion from this quantitative analysis is that the rate equation theory is still a reliable approximation for average quantities, despite the changes in the main kinetic mechanisms determining the evolution of large CZs and large islands (responsible for the crossover in the right tails of ISD and CZD).

Now we consider the deviations from PE behavior with increasing coverage. For instance, Fig. 3 shows that

the islands are very close (so, strongly correlated) for $R = 10^7$ and $\theta = 0.2$. They grow mainly by random aggregation of mass deposited near its branches, and not by capturing diffusing atoms that incided in island-free areas. Thus, there is significant increase in the widths of island branches when θ evolves to 0.3 and 0.4, instead of increase of the length of the branches (in other words, islands become less ramified).

This situation may also be viewed as a case of small average adatom diffusion lengths because the free area available is small. Again, rescaling of the lattice by $\langle l_D \rangle$ and of the time by $\langle t_D \rangle$ indicates that most atoms will aggregate immediately after incidence. This corresponds to RSA scaling.

It is worth to recall that an attempt to deposit an atom on an already occupied site is rejected in our models, and a new site is randomly chosen. However, in many simulation works, that atom is randomly aggregated in the island periphery. For low coverages, this condition is irrelevant, but for large coverages the second rule increases the number of static adatoms aggregated to islands. Thus, the crossover effects would be enhanced if this (more realistic) mechanism is used.

IV. DISTRIBUTIONS FOR SQUARE ISLANDS

We performed simulations of the square island model in the same range of parameters of the fractal island simulations.

In Figs. 5a and 5b, we show CZD for $R = 10^9$ and various coverages, in logarithmic and linear plots, respectively. The data for small coverage ($\theta = 0.1$) is well fitted by the WS, but deviations are large for $\theta = 0.25$

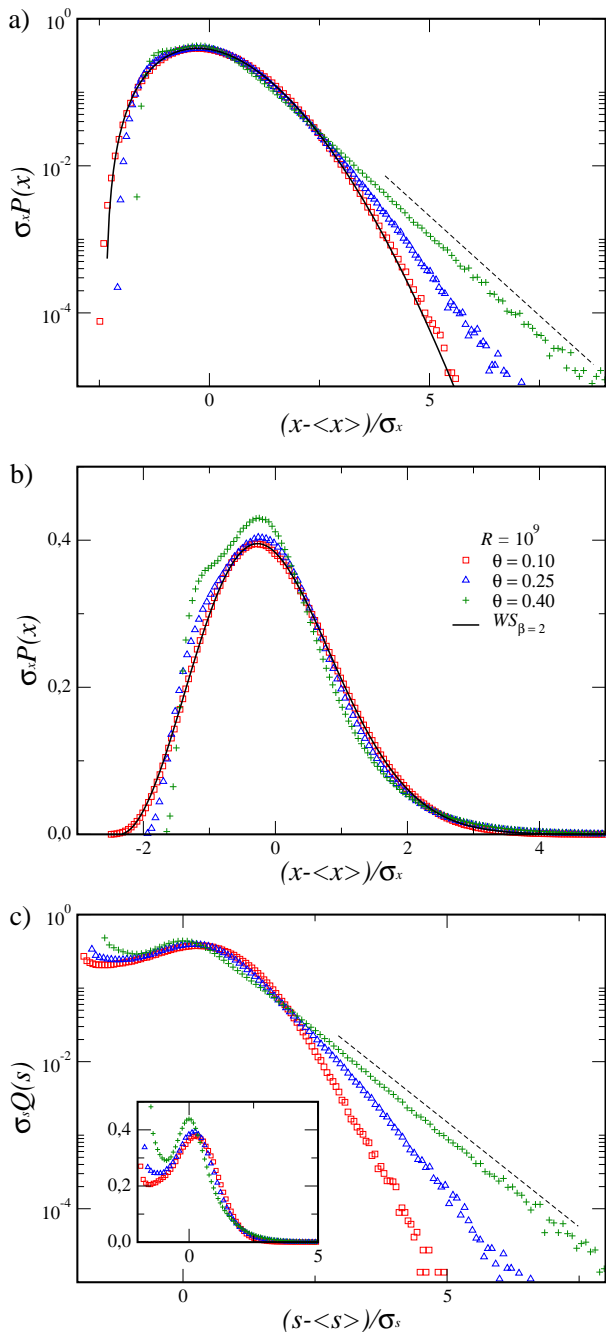


FIG. 5: (Color online) Scaled CZD (a,b) and ISD (c) for square islands with $i = 1$, $R = 10^9$ and several coverages. The solid line in (a) and (b) is the WS with $\beta = 2$. Dashed line in (a), (c) are guides to the eye.

and larger coverages. Again, the Gaussian decay of the right tail of the CZD (PE scaling) crosses over to simple exponential decay as θ increases.

In Fig. 5c, we show ISD for the same set of parameters, showing the crossover from the Gaussian decay (small coverage) to the simple exponential (large coverage). The inset of Fig. 5c highlights the small island densities.

Important differences from the fractal island case can

be noted in the distributions of Figs. 5a-c.

The first one is the presence of many small islands for all coverages, which was already noted in Ref.⁴⁴. For $\theta = 0.4$, the density of small islands ($s = 2, 3, 4$) is comparable to the density of islands of the average size ($s \approx 1100$). This certainly affects all results from continuous approaches, which is the case of the PE theory, and justifies the deviations between the CZD and the WS for relatively small coverages.

Another difference is the formation of a shoulder in the CZD as θ increases (Fig. 5b). This is also related to the presence of small islands. Despite their small size, their CZ areas are not small; instead, they are only slightly smaller than the most probable CZ areas (peaks of CZD).

Results for fixed coverage and decreasing R show the same crossover of the fractal islands (Figs. 2a and 2b). However, the simple exponential decay of the right tails (of CZD and ISD) appears for larger values of R , i. e. the Gaussian CZD is observed in a narrower range for square islands.

Fig. 6 shows images of the submonolayers grown with $R = 10^7$ and $R = 10^9$. For any coverage, the free areas around the square islands are larger than those around the fractal islands. Thus, one should expect PE theory to apply for larger coverages with square islands. However, the opposite occurs: deviations of the CZD from the WS appear for smaller coverages when compared to fractal islands.

The formation of small islands explains the deviations in the left tail and in the peak of CZD. On the other hand, the change in the right tail scaling (from Gaussian to simple exponential) is not explained by this feature, but is related to island coalescence. For $\theta = 0.2$, only two-island coalescence can be seen in Fig. 6 and is significant for $R = 10^7$. For $\theta = 0.4$, coalescence of many islands is noticeable for both values of R . Now suppose that the system is rescaled by a factor $\langle s \rangle$, so that an average island of the original system is converted to a single occupied site. After rescaling, the largest islands are formed by coalescence of some randomly distributed sites, which were the coalesced islands in the original system. Thus, ISD and CZD have right tails as in random distribution of occupied sites, i. e. RSA.

V. MODEL WITH DIFFUSION AND FREEZING ($i = 0$ CASE)

This model was introduced by Amar and Family⁶ to represent growth with critical island size $i = 0$ incorporating diffusion effects. That model is different from the random sequential adsorption (RSA), in which atoms irreversibly stick to the site where they are adsorbed, without diffusion^{24,25}.

In the model, the adatoms diffuse with coefficient D and stop moving (freeze and nucleate a new stable island) with rate $R_s = rD$, with $r \leq 1$. The freezing rate depends on an extra activation energy E_F as

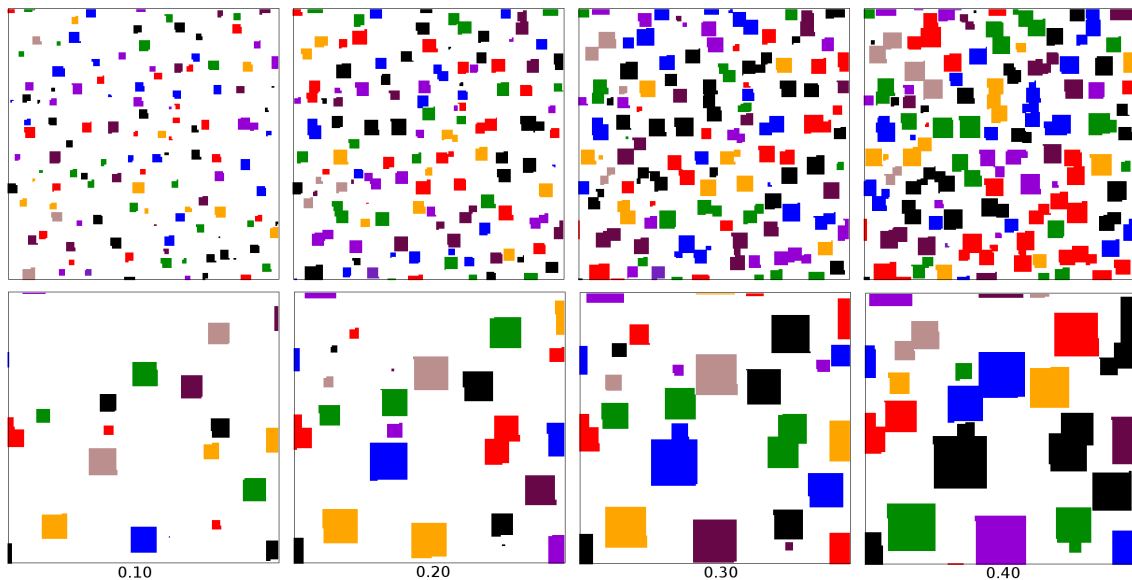


FIG. 6: (Color online) Square islands for several coverages with $R = 10^7$ (top) and $R = 10^9$ (bottom). The panels of lateral size 200 sites are cut from a system of size $L = 2048$.

$r = \exp(-E_F/k_B T)$, which may represent the effect of surfactants or impurities^{45,46}. Adatoms also stop moving when they become nearest neighbors of stable islands, producing islands with fractal shape. However, an adatom does not stop moving when it meets one or more diffusion adatoms, which is the main difference from the models with $i > 0$.

We performed simulations of this model in lattices of lateral size $L = 2048$, with R between 10^9 and 10^{11} , coverages up to $\theta = 0.3$, and r ranging from 10^{-2} to 10^{-5} .

In Figs. 7a and 7b we show scaled CZD and ISD, respectively, for different freezing rates and fixed R and θ . For $r = 10^{-5}$, the CZD shows a reasonable agreement with the PE theory for $i = 0$ (WS with $\beta = 1$). However, a large deviation is observed for $r = 10^{-3}$, where the tail decay is slower than a Gaussian (see inset of Fig. 7a). The ISD have simple exponential decay for $r = 10^{-3}$ and large s , again typical of RSA.

We notice that, in this model, islands are produced only by adatoms that stop moving. Thus, the number of islands increases with the rate r , decreasing the CZ areas and the size of the free regions between the islands.

The crossover in CZD can be explained by a comparison of CZ areas with the model with $i = 1$ (Sec. III).

The average CZ area for $r = 10^{-5}$ and $\theta = 0.1$ is $\langle x \rangle \approx 880$. Comparing with fractal islands grown with $i = 1$ and the same coverage, we note that this value is between the CZ area for $R = 10^7$ ($\langle x \rangle \approx 500$) and for $R = 10^8$ ($\langle x \rangle \approx 1200$). Both CZD agree with the WS with $\beta = 2$, as shown in Ref.¹² (see also Fig. 2a for $R = 10^8$). The case $R = 10^7$ is also illustrated in Fig. 3 and show large areas between the islands.

On the other hand, the average CZ area for $r = 10^{-3}$

and $\theta = 0.1$ is much smaller: $\langle x \rangle \approx 88$. This value is close to the average CZ area for fractal islands with $i = 1$, $\theta = 0.1$, and $R = 10^4$: $\langle x \rangle \approx 64$ (for $R = 10^5$, we find $\langle x \rangle \approx 120$). The corresponding CZD is shown in Fig. 2a and has significant deviation from the WS with $\beta = 2$.

The deviations from PE scaling for small R in fractal islands are related to the decrease of the average CZ area and the corresponding decrease in the available area between the islands. The crossover occurs for an average CZ area near 100 lattice sites, which apparently independes on the value of i , reinforcing the geometric argument.

The case $r = 1$ is equivalent to the RSA, since adatoms freeze with the same rate that they move to neighboring sites. Consequently, our results consistently illustrate a crossover from a regime of island growth from diffusing adatoms to a regime of island formation by approximately static adatoms.

VI. CONCLUSION

We simulated irreversible growth of fractal and square islands with critical island size $i = 1$ and 2, for several values of diffusion-to-deposition ratio R and coverage θ , and simulated a model with $i = 0$, with adatom diffusion and freezing. ISD and CZD were calculated and the crossover from PE theory predictions to different distribution shapes was analyzed, with a focus on the right tail decays.

For fractal islands, small θ and large values of R lead to Gaussian CZD, which is consistent with the PE theory. ISD have left tails slightly faster than Gaussian. However, as the island density increases (due to increas-

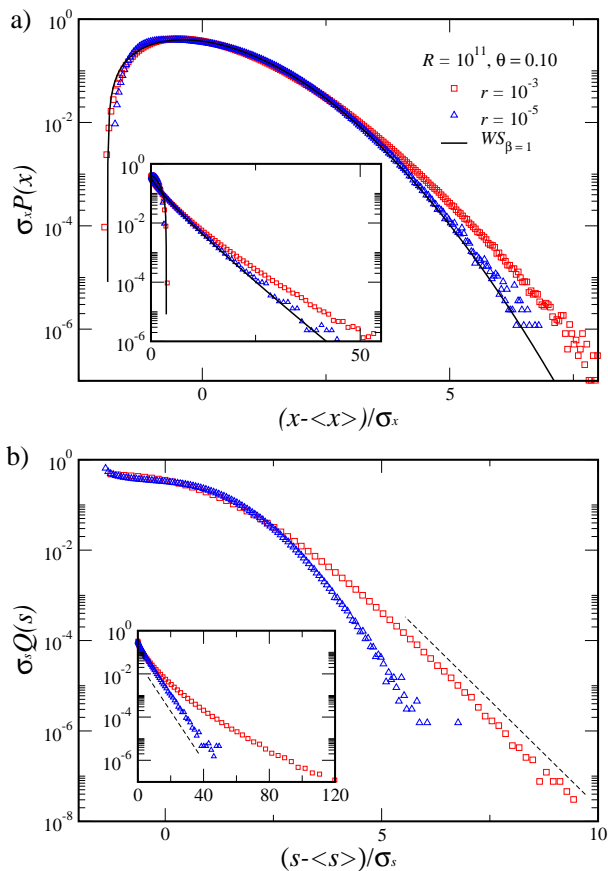


FIG. 7: (Color online) Scaled CSD (a) and ISD (b) for $i = 0$ model with $R = 10^{11}$, $\theta = 0.10$ and $r = 10^{-3}$ (squares, red) and $r = 10^{-5}$ (triangles, blue). The solid line is the WS with $\beta = 1$. The insets show the same distributions with abscissas $[(z - \langle z \rangle)/\sigma_z]^2$ in (a) and $[(s - \langle s \rangle)/\sigma_s]^2$ in (b).

ing θ or decreasing R), the area between neighboring islands becomes very small. This strong correlation between islands leads to a crossover to simple exponential decays of CSD and ISD. For small R or large θ , the deposited adatoms have very small diffusion lengths before

aggregating to a stable island, which is interpreted as a crossover to the problem of random distributions of static atoms (RSA problem). For fixed coverage, estimates of the island sizes and CZ areas at the crossover have R -scaling consistent with rate equation theory for $i = 1$ and $i = 2$.

For square islands, small θ and large values of R lead to Gaussian CZD and ISD. Compared to the fractal island case, the crossover is observed for smaller values of θ and larger values of R , despite the larger area between neighboring islands. In the square island case, the deviations from PE predictions is partially attributed to the presence of many small islands, whose densities are of the same order of the (much larger) average islands. However, the crossover from Gaussian to simple exponential decay in CZD and ISD is mainly related to coalescence of islands, since large islands and large CZs are effectively formed by random distribution of (static) rescaled islands.

In the model with diffusion and freezing, island shape is also fractal. For small values of the freezing rate r , islands are separated by large areas and the CZD obeys the PE theory for $i = 0$. As r increases, the area between the islands become very small, so that CZD and ISD get a simple exponential decay, similar to the fractal islands with $i = 1$.

The Gaussian tail of CZD and related forms of ISD are found only for small coverages (usually $\theta < 0.3$) and for large values of R , thus their experimental observation is probably difficult. Moreover, large values of R are characteristic of high temperatures, where the hypothesis of a critical (and small) island size may fail. This strongly suggests extensions of the theoretical and simulational study to reversible island growth and to systems with cluster diffusion, which were focus of recent work⁴⁷.

Acknowledgments

The authors acknowledge support from CNPq, FAPEMIG and FAPERJ (Brazilian agencies).

- ¹ J.W. Evans, P. A Thiel, and M. C. Bartelt, Surf. Sci. Rep. **61**, 1 (2006).
- ² A. Pimpinelli and J. Villain, *Physics of Crystal Growth* (Cambridge University Press, Cambridge, England, 1998).
- ³ *Frontiers in Surface and Interface Science*, edited by Charles B. Duke and E. Ward Plummer (Elsevier, Amsterdam, 2002).
- ⁴ J. A. Venables, *Introduction to Surface and Thin Film Processes* (Cambridge University Press, Cambridge, England, 2000).
- ⁵ C. Ratsch and J. A. Venables, J. Vac. Sci. Technol. **A 21**, S96 (2003).
- ⁶ J. G. Amar and F. Family, Phys. Rev. Lett. **74**, 2066 (1995).

- ⁷ P. A. Mulheran and J. A. Blackman, Philos. Mag. Lett. **72**, 55 (1995); Phys. Rev. B **53**, 10261 (1996).
- ⁸ A. Pimpinelli and T. L. Einstein, Phys. Rev. Lett. **99**, 226102 (2007).
- ⁹ F. Shi, Y. Shim, and J. G. Amar, Phys. Rev. E **79**, 011602 (2009).
- ¹⁰ M. Li, Y. Han, and J. W. Evans, Phys. Rev. Lett. **104**, 149601 (2010).
- ¹¹ A. Pimpinelli and T. L. Einstein, Phys. Rev. Lett. **104**, 149602 (2010).
- ¹² T. J. Oliveira and F. D. A. Aarão Reis, Phys. Rev. B **83**, 201405(R) (2011).
- ¹³ P. A. Mulheran, D. Pellenc, R. A. Bennett, R. J. Green, and M. Sperrin, Phys. Rev. Lett. **100**, 068102 (2008).

- ¹⁴ D. Choudhary, P. Clancy, R. Shetty, and F. Escobedo, *Adv. Functional Mater.* **16**, 1768 (2006).
- ¹⁵ R. Ganapathy, M. R. Buckley, S. J. Gerbode, and I. Cohen, *Science* **327**, 445 (2010).
- ¹⁶ J. H. Lloyd-Williams, B. Monserrat, D. D. Vvedensky, and A. Zangwill, *Phys. Rev. B* **85**, 161402(R) (2012).
- ¹⁷ B. R. Conrad, E. Gomar-Nadal, W. G. Cullen, A. Pimpinelli, T. L. Einstein, and E. D. Williams, *Phys. Rev. B* **77**, 205328 (2008).
- ¹⁸ M. A. Groce, B. R. Conrad, W. G. Cullen, A. Pimpinelli, E. D. Williams, and T. L. Einstein, *Surf. Sci.* **606**, 53 (2012).
- ¹⁹ M. L. Mehta, *Random Matrices* (Academic, New York, 2004), 3rd ed; T. Guhr et al, *Phys. Rep.* **299**, 189 (1998).
- ²⁰ D. L. González, A. Pimpinelli, and T. L. Einstein, *Phys. Rev. E* **84**, 011601 (2011).
- ²¹ M. Grinfeld, W. Lamb, K. P. O'Neill, and P. A. Mulheran, *J. Phys. A: Math. Theor.* **45**, 015002 (2011).
- ²² K. P. O'Neill, M. Grinfeld, W. Lamb, and P. A. Mulheran, *Phys. Rev. E* **85**, 021601 (2012).
- ²³ D. L. González and T. L. Einstein, *Phys. Rev. E* **84**, 051135 (2011).
- ²⁴ V. Privman, *Colloids Surf. A* **165**, 231 (2000).
- ²⁵ J. W. Evans, *Rev. Mod. Phys.* **65**, 1281 (1993).
- ²⁶ R. Ruiz, B. Nickel, N. Koch, L. C. Feldman, R. F. Haglund, Jr., A. Kahn, F. Family, and G. Scoles, *Phys. Rev. Lett.* **91**, 136102 (2003).
- ²⁷ Y. Wu, T. Toccoli, N. Koch, E. Iacob, A. Pallaoro, P. Rudolf, and S. Iannotta, *Phys. Rev. Lett.* **98**, 076601 (2007).
- ²⁸ J. Shi and X. R. Qin, *Phys. Rev. B* **78**, 115412 (2008).
- ²⁹ H. Zheng, M. H. Xie, H. S. Wu, and Q. K. Xue, *Phys. Rev. B* **77**, 045303 (2008).
- ³⁰ S. Lorbek, G. Hlawacek, and C. Teichert, *Eur. Phys. J. Appl. Phys.* **55**, 23902 (2011).
- ³¹ T. Potocar, S. Lorbek, D. Nabok, Q. Shen, L. Tumbek, G. Hlawacek, P. Puschnig, C. Ambrosch-Draxl, C. Teichert, and A. Winkler, *Phys. Rev. B* **83**, 075423 (2011).
- ³² R. Sathiyarayanan, A. B. Hamouda, A. Pimpinelli, and T. L. Einstein, *Phys. Rev. B* **83**, 035424 (2011).
- ³³ F. Arciprete, M. Fanfoni, F. Patella, A. Della Pia, A. Balzarotti, and E. Placidi, *Phys. Rev. B* **81**, 165306 (2010).
- ³⁴ T. A. Witten and L. M. Sander, *Phys. Rev. Lett.* **47**, 1400 (1981).
- ³⁵ M. C. Bartelt, J. W. Evans, *Surf. Sci.* **298**, 421 (1993).
- ³⁶ T. J. Oliveira and F. D. A. Aarão Reis, *Phys. Rev. E* **76**, 061601 (2007).
- ³⁷ T. J. Oliveira and F. D. A. Aarão Reis, *J. Appl. Phys.* **101**, 063507 (2007).
- ³⁸ M. Körner, M. Einax, and P. Maass, *Phys. Rev. B* **82**, 201401(R) (2010).
- ³⁹ P. Meakin, *Phys. Rev. A* **27**, 604 (1983).
- ⁴⁰ D. Stauffer and A. Aharony, *Introduction to Percolation Theory*, 2nd. edition (Taylor & Francis, London/Philadelphia, 1992).
- ⁴¹ J. A. Venables, *Phyl. Mag.* **27**, 697 (1973).
- ⁴² J. A. Venables, G. D. Spiller, and M. Hanbuchen, *Rep. Prog. Phys.* **47**, 399 (1984).
- ⁴³ S. Stoyanov and K. Kashchiev, *Curr. Top. Mat. Sci.* **7**, 69 (1981).
- ⁴⁴ M. C. Bartelt and J. W. Evans, *Surf. Sci.* **298**, 421 (1993).
- ⁴⁵ G. Rosenfeld, R. Servaty, C. Teichert, B. Poelsema, and G. Comsa, *Phys. Rev. Lett.* **71**, 895 (1993).
- ⁴⁶ D. D. Chambliss and K. E. Johnson, *Phys. Rev. B* **50**, 5012 (1994).
- ⁴⁷ Y. A. Kryukov and J. G. Amar, *Phys. Rev. E* **83**, 041611 (2011); B. C. Hubartt, Y. A. Kryukov, and J. G. Amar, *Phys. Rev. E* **84**, 021604 (2011).